The Astronomical Journal, 133:1690–1697, 2007 April
© 2007. The American Astronomical Society. All rights reserved. Printed in U.S.A.

ISO-CHA I 192: A NEW EMBEDDED ERUPTIVE VARIABLE IN THE CHAMAELEON I DARK CLOUD[1]

P. Persi
Istituto Astrofisica Spaziale e Fisica Cosmica, INAF, Roma, Italy; paolo.persi@iasf-roma.inaf.it

M. Tapia
Instituto de Astronomía, Universidad Nacional Autónoma de México, Ensenada, Baja California, Mexico; mt@astrosen.unam.mx

M. Gòmez
Observatorio Astronómico de Córdoba, Córdoba, Argentina; mercedes@oac.uncor.edu

B. A. Whitney
Space Science Institute, Boulder, CO, USA; bwhitney@spacescience.org

A. R. Marenzi
Istituto Astrofisica Spaziale e Fisica Cosmica, INAF, Roma, Italy; annarosa.marenzi@iasf-roma.inaf.it

and

M. Roth
Las Campanas Observatory, Carnegie Institution of Washington, La Serena, Chile; miguel@lco.cl
Received 2006 August 11; accepted 2006 December 1

ABSTRACT

We report the detection of an increase of about 2 mag in the 2.2 μm brightness of ISO-Cha I 192, a class I low-mass stellar object thought to be driving a bipolar CO outflow in the Chamaeleon I cloud. This substantial brightness change has taken place during less than 3 yr, from 1996 March to 1999 April. An elongated infrared reflection nebula of size $\sim$530 AU is seen originating from the star in the direction of the CO bipolar outflow. The historic infrared properties of this young stellar object are examined in order to substantiate the hypothesis that this object is an FU Ori– or EX Lup–type system. Combining our new ground-based near- and mid-infrared photometry with *Spitzer* IRAC and MIPS broadband fluxes supplemented by published recent spectrophotometry, the spectral energy distribution of this source was constructed. We explored the plausibility of a "standard" configuration of infalling envelope + disk + central source for this object by fitting a two-dimensional radiative transfer code that includes the contributions of each of these components.

Key words: circumstellar matter — ISM: individual (Chamaeleon I) — ISM: jets and outflows — stars: formation — stars: low-mass, brown dwarfs — stars: pre–main-sequence

1. INTRODUCTION

ISO-Cha I 192, also referred to in the literature as [CCE98] 2-41, DENIS-P J1109.5−7633 (Cambrésy et al. 1998), [PMK99] ISOCAM Cha I-Na2 (Persi et al. 1999), and [PMK99] IR Cha I-Na1 (Gómez & Mardones 2003), is a young class I member of the Chamaeleon I dark cloud, with no optical counterpart detected so far. Based on the relatively uncertain spectral type (M3.5–M6.5) derived by Gómez & Mardones (2003) and its location in the H-R diagram and in D'Antona & Mazzitelli's (1994) evolutionary tracks, an age ranging from 2×10^5 to 3×10^6 yr has been estimated by these authors for this star. From their crude extinction map of the area, Jones et al. (1985) estimated $A_V \geq 13$ in the direction of this object ($\alpha = 11^{\rm h}09^{\rm m}29.4^{\rm s}$, $\delta = -76^{\rm o}33'28''$ [J2000.0]), and Mizuno et al. (1999) detected a dense $C^{18}O$ core in this area. Persi et al. (1999), on the other hand, identified ISO-Cha I 192 as the driving source of a large-scale ^{12}CO (1–0) outflow in the region (Mattila et al. 1989). Gómez et al. (2004) found five H_2 knots that roughly align with the CO outflow direction.

In this contribution we report a brightness increase in ISO-Cha I 192 of around 2 mag in the K_s band from 1996 to 1999, similar to that exhibited by a number of FU Orionis variables (FUors; see, e.g., Hartmann & Kenyon 1996) or EXors (EX Lupi being the prototype of this group; Herbig 1977; Herbig et al. 2001). In § 2 we present new photometry of this object from archive *Spitzer* IRAC and MIPS images added to that obtained from our La Silla and Las Campanas observations. In § 3 we combine these data with those from the literature to construct a crude K_s-band light curve, use an image-enhancing technique to study the properties of an associated reflection nebula, and construct a nearly simultaneous spectral energy distribution (SED) of ISO-Cha I 192. We also attempt to fit a model to quasi-simultaneous photometric points in order to explore the plausibility of a "standard" configuration of infalling envelope + disk + central source for ISO-Cha I 192 using the radiative transfer code of Whitney et al. (2003b). In § 4 we provide arguments in favor of considering this object a young FUor or EXor system. Finally, we present a brief summary in § 5.

2. OBSERVATIONS

ISO-Cha I 192 was observed on the night of 2003 May 15 using Persson's Auxiliary Nasmyth Infrared Camera (PANIC) attached to the Magellan Clay 6.5 m telescope at Las Campanas Observatory (Chile). PANIC has a Rockwell 1024×1024 Hawaii array that provides a $2' \times 2'$ field of view with $0.125''$ pixel^{-1}. We used the K_s filter, with a bandwidth of 0.32 μm, and obtained nine

[1] Based on observations collected at the European Southern Observatory, La Silla, Chile, ESO proposal 073.C-0099(A), and at Las Campanas Observatory, Chile.

TABLE 1
ISO-Cha I 192 Observed Flux Densities and Observation Details

Wavelength (μm)	Flux (Jy)	Julian Date	Instrument/Telescope
2.2 (K_s)	0.038 ± 0.001	2,452,775	PANIC/Clay
3.6	0.12 ± 0.01	2,453,191	IRAC/*Spitzer*
4.5	0.29 ± 0.02	2,453,191	IRAC/*Spitzer*
5.8	0.54 ± 0.03	2,453,191	IRAC/*Spitzer*
8.0	0.85 ± 0.04	2,453,191	IRAC/*Spitzer*
8.9	0.80 ± 0.11	2,453,097	TIMMI2/ESO 3.6 m
9.8	0.55 ± 0.07	2,453,097	TIMMI2/ESO 3.6 m
12.9	1.15 ± 0.09	2,453,097	TIMMI2/ESO 3.6 m
71	12.3 ± 1.2	2,453,107	MIPS/*Spitzer*

dithered frames of 5 s, offsetting the telescope by 6″ between consecutive exposures. The measured point-spread function (PSF) full width at half-maximum (FWHM) was about 0.8″. As discussed in § 3, ISO-Cha I 192 appears clearly extended. We also observed a few standards from the list of Persson et al. (1998) to calibrate the data. It is important to note that the photometry of the nearby star [CCE98] 40 from our Magellan telescope image, $K_s = 10.24$ (see Fig. 2), is in reasonable agreement with that published for the same object by Cambrésy et al. (1998), $K_s = 10.11$.

Mid-infrared images of ISO-Cha I 192 were obtained on 2004 April 1, with the mid-infrared camera Thermal Infrared Multi-Mode Instrument 2 (TIMMI2) attached to the 3.6 m ESO telescope at La Silla (Chile). TIMMI2 uses a 320 pixel × 240 pixel Si:As array manufactured by Raytheon, providing a field of view of 64″ × 48″ for the 0.2″ pixel^{-1} magnification lens. We observed this source with narrowband filters centered at 8.9, 9.8, and 12.9 μm, having bandwidths of 0.78, 0.93, and 1.18 μm, respectively.

The images were taken using the standard chop-nodding technique to correct for the background. We employed a chop throw of 10″, with a nodding offset of 10″ perpendicular to the chop direction. The central 300 pixel × 220 pixel area of the detector were used to register the data. Both the positive and negative images were combined to construct the final images in each band. This was done by shifting and adding all the sources in each chop-nod frame. The total on-source integration time was equivalent to 30 minutes at 12.9 μm and 24 minutes at 9.8 and 8.9 μm.

The photometry was calibrated with a number of TIMMI2 standard stars as listed in the TIMMI2 user's manual,[2] which were observed at an air mass similar to that of our source. The derived PSFs (FWHM) were 1.26″, 1.32″, and 1.24″ at 8.9, 9.8, and 12.9 μm, respectively. A detection limit (2 σ) of about 1 mJy pixel^{-1} in all three filters was obtained. No evidence of extended emission around ISO-Cha I 192 was found in these images. The nearby star [CCE98] 40 was too faint to be detected in any of these images.

The star ISO-Cha I 192 lies in one of the fields included in the *Spitzer Space Telescope* program "Structure and Incidence of Young Embedded Clusters" (PI: G. Fazio), for which IRAC (3.6, 4.5, 5.8, and 8 μm) and MIPS (24 and 71 μm) calibrated images were obtained and are now available in the science archive. ISO-Cha I 192 was saturated in the 24 μm image. The IRAC images, taken in IRAC-MAP mode, have a scale of 1.22″ pixel^{-1}, and that from MIPS, at 71 μm, taken in SCAN-MODE, has 9.98″ pixel^{-1}. ISO-Cha I 192 was unresolved in all bands. Photometry of ISO-Cha I 192 was obtained from the IRAC images using a 3 pixel aperture and a background annulus of 3–7 pixels. Aperture correction was applied according to the values given in the IRAC user manual. The MIPS photometry was obtained with a radius of 3.55 pixels and a background annulus of 4.0–6.6 pixels. Aperture correction was also applied according to the MIPS manual.

The measured flux densities for the star ISO-Cha I 192 at all observed wavelengths are listed in Table 1, which also gives the dates of observation. Integrating the SED between 1.2 and 70 μm, we obtain $F_{(1-70)} = 2.45 \times 10^{16}$ W cm^{-2}. For a distance of 160 pc, this corresponds to a luminosity of $L_{\rm IR} = 1.5\ L_{\odot}$.

3. RESULTS

3.1. *Infrared Variability*

Table 2 lists the available J, H, and K_s magnitudes for this source, together with the dates of the observations compiled from the literature and determined from our Magellan K_s image. Figure 1 shows the corresponding light curve. This plot includes 13 individual observations obtained in about a 3 month period (early 2000) as part of the Two Micron All Sky Survey (2MASS; Carpenter et al. 2002). The mean value of these is reported in the corresponding entry in Table 2. Note that the quoted magnitude from Gómez & Kenyon (2001) corresponds to the K band instead of the K_s band, as is the case for the rest of the data.

To derive the K_s magnitude for 1999 April 12 (see Table 2 and Fig. 1), we integrated the near-infrared spectrum obtained by Gómez & Mardones (2003) throughout the 2MASS K_s bandpass. The spectrum of the companion star [CCE98] 40 (see Fig. 2) was obtained simultaneously with that of ISO-Cha I 192, since both objects lie on the slit. We used the 2MASS K_s magnitude of [CCE98] 40 (10.25) to calibrate the K_s-band magnitude of ISO-Cha I 192. We caution, however, that, since this is not a true photometric measurement, the uncertainties are larger than the other values quoted in Table 2.

[2] At http://www.ls.eso.org/lasilla/Telescopes/360cat/timmi/html/uman/LSO-TIMMI-MAN.html.

TABLE 2
Photometry of ISO-Cha I 192 and Dates of Observation

Date	Julian Date	K_s	H	J	Reference
1996 Jan 21	2,450,103	12.24	...	...	DENIS, Cambrésy et al. (1998)
1996 Mar 1–3	2,450,144–2,450,146	12.22	14.59	17.52	Oasa et al. (1999)
1996 Mar 3–4	2,450,146–2,450,147	12.75	15.28	18.24	Persi et al. (1999)
1996 Mar 11	2,450,154	12.18[a]	14.59	17.92	Gómez & Kenyon (2001)
1999 Apr 12	2,451,279	11[b]	...	...	This paper
2000 Jan–Mar	2,451,545–2,451,635	11.02	13.27	16.07	2MASS, Carpenter et al. (2002)
2003 May 15	2,452,775	10.61	...	...	This paper

[a] K band instead of K_s magnitude.
[b] Estimated K_s magnitude from the spectrum obtained by Gómez & Mardones (2003).

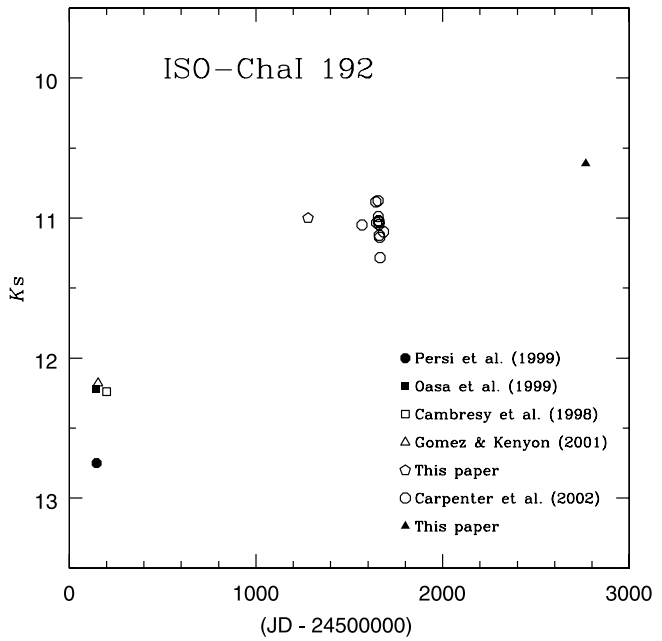

FIG. 1.—ISO-Cha I 192 K_s-band light curve from 1996 September to 2003 July. The values of the photometry are listed in Table 2.

In ISO-Cha I 192, we find evidence of small-amplitude ($\Delta K_s \sim 0.5$) variability on timescales of days, apart from a large increase in brightness ($\Delta K_s \geq 2$) that was found to occur in a period of less than 3 yr, from 1996 March to 1999 April, as can be seen in Figure 1. There are no observations of this star prior to 1996 or after 2003 available in the literature; thus, the light curve in Figure 1 does not necessarily register the total amplitude of the variation experienced by this source. Clearly, this light curve does not provide direct information about the actual timescale of the outburst, as it might have occurred in a rapid manner (e.g., 100 days) anytime between mid-1996 and early 1999. We cannot rule out, however, a slower brightness increase.

From the short-wavelength data in Table 2, we can only state that the observed 2.2 μm variations seem to be mimicked in the J and H bands. With the extremely limited data available in the mid-infrared range (from the *Infrared Space Observatory* [*ISO*] and *Spitzer*), the assessment of variability at these wavelengths can only be tentative. Fluxes at $\lambda = 6.7$ and 14.3 μm have been reported by Persi et al. (1999) based on ISOCAM calibrated images taken in 1996 April, most likely before ISO-Cha I 192 went into outburst ($F_{6.7\,\mu\mathrm{m}} = 0.22$ Jy and $F_{14.3\,\mu\mathrm{m}} = 1.41$ Jy). Postoutburst fluxes at these wavelengths can be derived by interpolating the observed 2004 mid-infrared photometric data from TIMMI2 and from IRAC and MIPS on *Spitzer* (Table 2), yielding $F_{6.7\,\mu\mathrm{m}} \simeq 0.7$ Jy and $F_{14.3\,\mu\mathrm{m}} = 2.1$ Jy. These values imply flux increases from 1996 to 2004 of approximately factors of 3.1 and 1.5 at 6.7 and 14.3 μm, respectively. Given the small quoted uncertainties in the flux determinations from both the *ISO* and *Spitzer* data, even allowing for the interpolation process in the latter, there is no reason to believe that these variations are not real.

Short-timescale variations in the visible and near-infrared are common among T Tauri stars and are usually attributed to the presence of cool and/or hot spots on the surface of these objects (Herbst et al. 1994; Batalha et al. 1998; Carpenter et al. 2002). However, the amplitude of this kind of variability in ISO-Cha I 192 is larger than is typically observed in T Tauri stars ($\Delta K_s \lesssim 0.2$; see, e.g., Skrutskie et al. 1996). Large-scale variations, like the one reported here for ISO-Cha I 192, are characteristic of eruptive variables of the FU Ori type and of EXors, although most of these are documented only in the optical. The amplitude of the present large K_s-band variation in ISO-Cha I 192 is similar to that shown by V1647 Ori, a candidate member of the FUor or EXor classes (Briceño et al. 2004; Aspin et al. 2006). This young stellar object that illuminates McNeil's Nebula has been reported to have suffered, between 1998 and 2004, a K-band brightness increase of about 3 mag (Reipurth & Aspin 2004), although this event most probably happened simultaneously with the outburst reported in the I_C band (Briceño et al. 2004) between 2003 January and 2004 February. Note that the shape of the light curve presented by these authors suggests that the photometric rise probably lasted less than 6 months. A similar outburst occurred in 1966–1967, as recently documented by Aspin et al. (2006), indicating that in V1647 Ori this is a recurrent phenomenon with (at least in this case) a period of 37 years.

3.2. *Extended Nebulosity*

Figure 2 shows direct images in the 2 μm atmospheric window of the region containing ISO-Cha I 192 and its companion star [CCE98] 40 corresponding to different epochs and taken with different instruments and telescopes. With the exception of the 2MASS frame, the spatial resolution (the FWHM of the stars the field) is less than 0.9″. In these cases, the morphology of ISO-Cha I 192 differs from the PSF. This is particularly clear in the 1996 duPont frame, in which the star itself was fainter.

In order to enhance the structure of the faint extended diffuse emission masked by the star, we subtracted the PSF, defined as the point-like image of the nearby star [CCE98] 40, from that of ISO-Cha I 192. For this, in each available image, we shifted the image so that the position of the star [CCE98] 40 exactly coincides with that of ISO-Cha I 192 in the original frame. After normalizing the shifted image so as to have the wings of the Gaussian of both stars at the same level, we subtracted one from the other. The results are shown in Figure 3 for six independent images, some taken through narrowband filters isolating the Brγ and 2.12 μm H_2 lines and also one centered at 2.09 μm showing only the narrowband continuum. The other two are broadband K_s images taken 7 yr apart. The elongated emission in the southeast-northwest direction and arising from ISO-Cha I 192 is clear. The orientation is coincident with that of the CO bipolar outflow.

As a test of the validity of this method, we repeated the same procedure using a number of much fainter, more distant stars in the field as PSF estimators, obtaining the same structures (with larger residuals, as expected) when subtracted from ISO-Cha I 192. No extended structure was seen at all when the PSF was subtracted from [CCE98] 40. Gómez et al. (2004) have presented some of these images. It must be added that the experiment was also carried out for the 2MASS images and the 3.6 and 4.5 μm IRAC images. As expected, after subtracting the PSF no trace of the extended nebulosity was seen on either of these, because of their low spatial resolution (∼2″).

The similarities in shape, orientation, length, and relative brightness of the extended structure arising from ISO-Cha I 192 are evident in all these images. Quantitatively speaking, on *all* these images we measured the same position angle (325° ± 2°) and length (∼3.3″ ± 0.2″ or 528 ± 30 AU) from ISO-Cha I 192 to the northwestern tip of the detectable nebulosity. Finally, the measured ratio of the flux density of the central star to that at the center of the nebulosity at a distance of 2.4″ from ISO-Cha I 192 was found in all images to be 151 ± 23, with the large dispersion caused by the rather low signal-to-noise ratio in the PSF-subtracted image of the elongated nebula. There was no indication whatsoever that the relative signal from the nebulosity was different in any

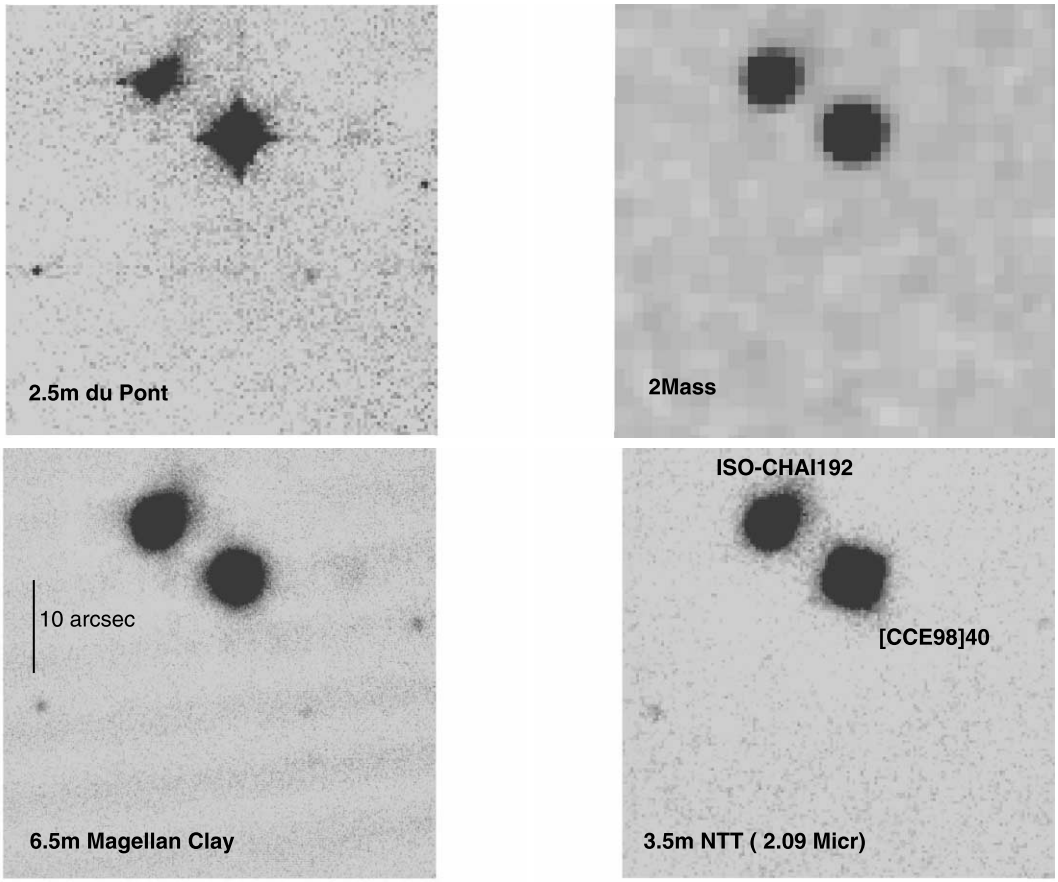

FIG. 2.—Direct images of the region containing ISO-Cha I 192 taken on different dates and with different telescope/instrument combinations. *Top left*: 1996 March 3–4, K_s band. *Top right*: 2000 January–March, K_s band. *Bottom left*: 2003 May 3, K_s band. *Bottom right*: 2003 April 17–18, 2.09 μm filter.

of the lines compared to that of the K_s continuum. This leaves no doubt that the diffuse elongated radiation comes from a reflection nebula.

That this extended nebulosity is mostly reflected light from the star may be a surprising result, given that the 2 μm spectrum of ISO-Cha I 192 taken in 1999 by Gómez & Mardones (2003) shows prominent H_2 line emission, including the 2.12 and 2.23 μm and the Q lines, over a rising, otherwise featureless continuum. Clearly, the H_2 lines must originate very close to the star. Note that the several knots of shocked H_2 emission are seen at distances of tens of arcseconds roughly along the CO flow. A discussion on the details of this flow and the association of this system with these H_2 emission knots is given by Gómez et al. (2004).

The ISO-Cha I 192 near-infrared nebulosity and variations resemble those associated with the previously known embedded FUors/EXors PP 13S (Tapia et al. 1997; Sandell & Aspin 1998), AR 6A/6B (Aspin & Reipurth 2003), OO Ser (Hodapp et al. 1996), and the Braid Nebula in the Cyg OB7 association (Movsessian et al. 2006). The presence of optical and/or near-infrared nebulae around FUors and EXors is one of the characteristics of these classes (see, e.g., Hartmann & Kenyon 1996; Herbig et al. 2001). On the other hand, it must be mentioned that our TIMMI2 mid-infrared images of ISO-Cha I 192 do not show an extended morphology (PSF $\sim 1.3''$).

3.3. *Spectral Energy Distribution*

Combining the available and nearly simultaneous near-, mid-, and far-infrared observations, we have constructed the SED of ISO-Cha I 192, plotted in Figure 4. The infrared fluxes obtained with *Spitzer*, TIMMI2, and PANIC were taken in a period that spans less than 13 months. Considering that there is evidence that the mid- and far-infrared flux variations are much smaller than in the visible, it is reasonable to assume that these data produce a good representation of the true SED of ISO-Cha I 192 for 2004, after its outburst. Note that the plotted values of J and H are extrapolated to 2003 May (the epoch of the K_s Clay observation) from the observed light curves at those wavelengths. Therefore, these values are more uncertain than for K_s. For the sake of completeness, our SED also includes the 3–4 μm fluxes from the Very Large Telescope spectrum reported by Pontoppidan et al. (2003), although this was taken in mid-2002. On the contrary, we omit the ISOCAM mid-infrared fluxes at 6.7 and 14.3 μm (Persi et al. 1999) because these were obtained about 6 yr before *Spitzer* and TIMMI2 observations (but see § 3).

In order to test the plausibility of a standard configuration consisting of an infalling envelope + disk + central source to describe this object, we fitted a model of this kind to the SED shown in Figure 4. The model we applied uses the two-dimensional radiation transfer code developed by Whitney et al. (2003b). Considering the limited number of data points and that we lack critical measurements at $\lambda > 70$ μm, we point out that this exercise must be taken as an experiment rather than a rigorous or precise determination of the physical and geometrical properties of this system.

To carry out our experiment, we defined a set of fixed parameters and a group of five free parameters. For the disk scale height at R_*, H, the radial density exponent A [$n(r) \propto r^{-A}$], and the scale height exponent B [$Z(h) \propto r^B$], we assumed standard values for T Tauri disks (i.e., 0.01, 1.875, and 1.125, respectively; see, e.g.,

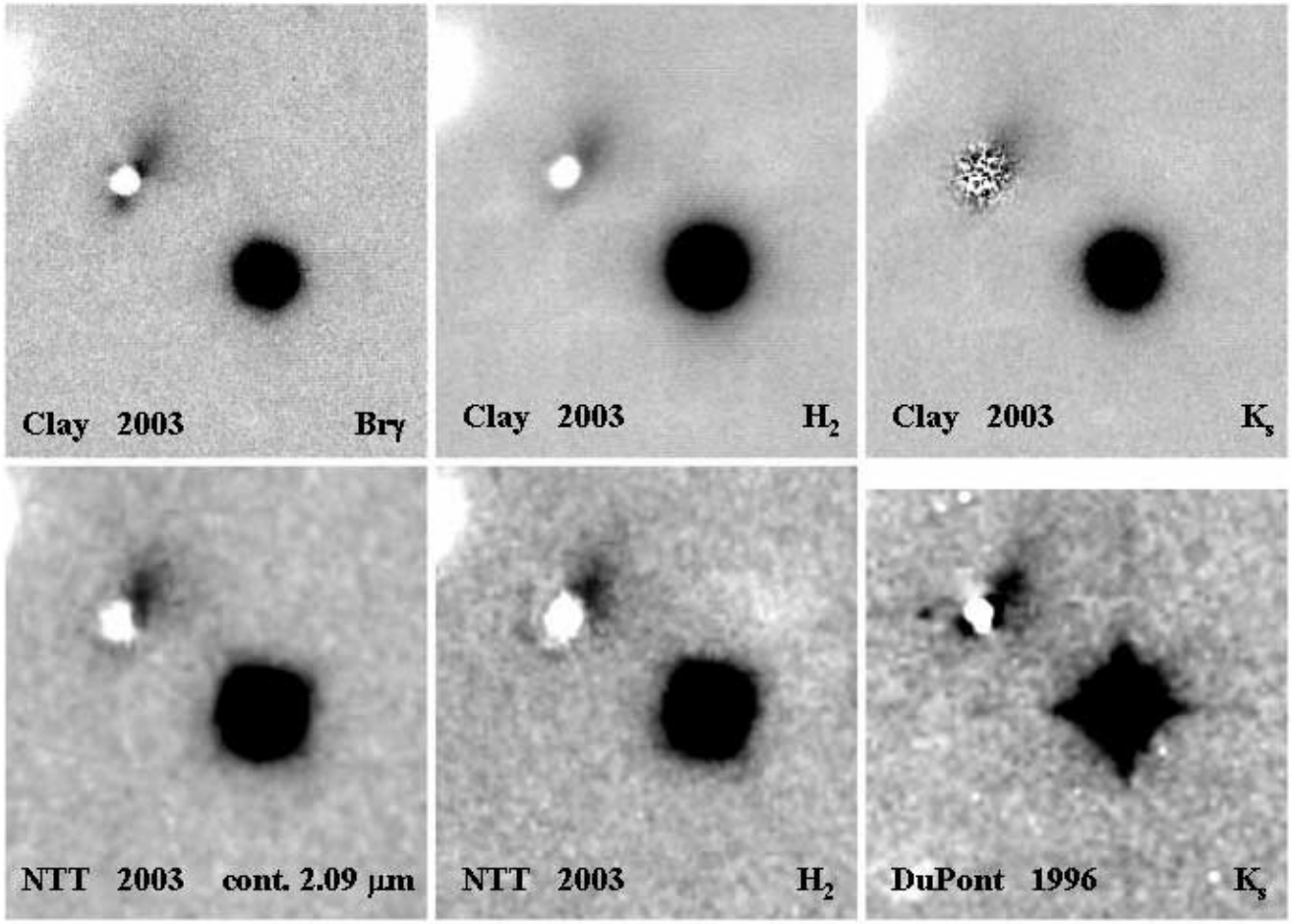

FIG. 3.—The $19'' \times 21''$ broadband and narrowband masked images of the region showing the morphology of the elongated reflection nebulosity around ISO-Cha I 192. These were taken through filters centered in the Brγ and 2.12 μm H_2 lines and the 2.09 μm continuum, as well as the K_s band. In all panels, the normalized PSF, defined as that of the nearby star [CCE98] 40, was subtracted from ISO-Cha I 192. The bright (*black*) spot represents [CCE98] 40, and the noisy (*top right*) and white (*other panels*) circles represent the residuals of the PSF subtraction at the position of ISO-Cha I 192 (see § 3.2 for details). The scale and orientation (north at top, east to the left) are identical for the six panels. The distance between ISO-Cha I 192 and [CCE98] 40 is $10''$.

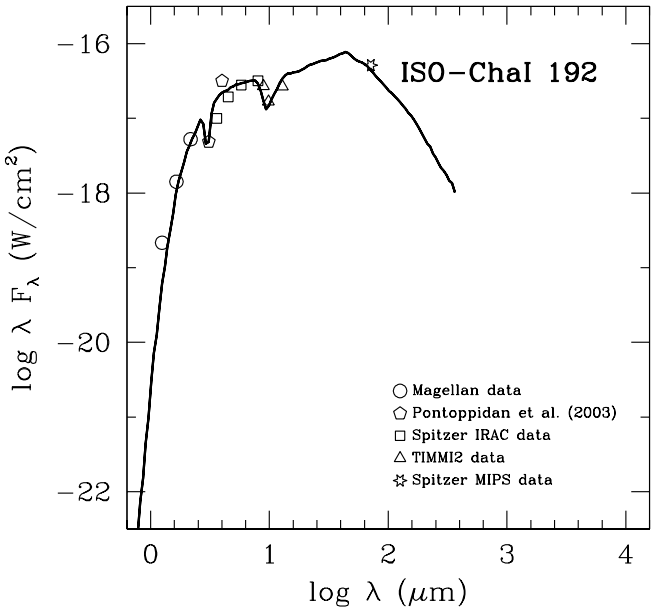

FIG. 4.—Observed 2003–2004 SED of ISO-Cha I 192. The solid line represents the best fit of the disk + envelope model (see text). The errors are estimated to be similar to the size of the symbols, except those derived from the spectrum by Pontoppidan et al. (2003; *pentagons*), which are estimated to be larger.

Kenyon & Hartmann 1987; Cotera et al. 2001). We also adopted a disk mass of 0.15 $M_\odot$, which is higher than for "typical" T Tauri disks ($\sim$0.05 $M_\odot$; see, e.g., Beckwith et al. 1990; Osterloh & Beckwith 1995; Andrews & Williams 2006) but in good agreement with submillimeter disk mass determinations for other previously known FUors and EXors (Sandell & Weintraub 2001). The inner radius of the disk ($R_{\rm gap} = 5.5R_*$) was set equal to the dust destruction or sublimation radius for the effective temperature $T_{\rm eff}$ of the central star. In addition, the magnetosphere corotating radius $R_{\rm trunc}$ was set to $5R_*$, since Kenyon et al. (1996) predict truncation radii of $2R_*$–$7R_*$ for typical magnetic field strengths and accretion rates of T Tauri stars (see also Stassun & Wood 1999). The size of the envelope, $R_{\rm env} = 3000$ AU, was fixed to a "common" value found in class I envelopes (Padgett et al. 1999; Reipurth et al. 2000; Hogerheijde & Sandell 2000; Jorgensen et al. 2002). In the infall model, material in the envelope is falling in to R_c. At first approximation, it seems reasonable to set an outer radius of the disk, $R_{\rm disk}$, equal to the falling-in radius (R_c). Also fixed were the stellar parameters, $R_* = 2.5\ R_\odot$, $M_* = 0.55\ M_\odot$, and $T_{\rm eff} = 3600$ K. These were chosen to represent an "average" T Tauri star with a bolometric luminosity comparable to that inferred from the direct observations (see § 2).

In the model, we allowed variations of the grain properties in different zones (disk midplane, disk atmosphere, envelope, and cavity) as described in Whitney et al. (2003a). To reproduce the

TABLE 3
ISO-Cha I 192: Free Parameters of the Model

Parameter	Value
$\dot{M}_{\rm disk}$ ($M_\odot$ yr^{-1})	$(1-2)\times10^{-7}$
$\dot{M}_{\rm env}$ ($M_\odot$ yr^{-1})	$(1-3)\times10^{-6}$
$R_c = R_{\rm disk}$ (AU)	5–20
θ (deg)	5–30
i (deg)	35–45

water ice feature at 3.1 μm we included a mantle of water ice on each dust grain, covering the outer 10% and 5% of the radii of the grains that are in the envelope and in the cavity, respectively. For the ambient cloud density $\rho_{\rm amb} = 1.67\times10^{-20}$ g cm^{-3} and the cavity density $\rho_{\rm cavity} = 1.67\times10^{-19}$ g cm^{-3}, the adopted values are typical for dense clouds and molecular outflows, respectively (see Whitney et al. 2003b). Finally, a polynomial shape for the cavity with an exponent 0.7 was adopted.

The group of free parameters includes the centrifugal radius R_c, the infalling rate $\dot{M}_{\rm env}$, the mass accretion of the disk $\dot{M}_{\rm disk}$, the cavity opening angle θ, and the inclination angle i. Table 3 gives the range of values for each of the free parameters for which we obtained fits of comparable quality to the observed data. The solid line in Figure 4 shows the model that corresponds to the mean values of the parameters listed in Table 3. The emergent star + disk + envelope flux was extincted following the mean interstellar extinction law, assuming a value of the optical extinction, $A_V = 13$, in reasonably good agreement with previous determinations of the extinction in this specific region of the cloud (Jones et al. 1985; Persi et al. 1999; Kainulainen et al. 2006). This model yields $L_{\rm total} = 1.55\ L_\odot$, including the stellar + accretion disk luminosity, since envelope accretion luminosity is negligible. The value is slightly larger than that obtained by integrating the SED (see § 2).

The derived disk accretion rate, $\dot{M}_{\rm disk} \sim 10^{-7}\ M_\odot$ yr^{-1} is, however, about 3 orders of magnitude lower than that estimated for posteruption class II FUor disks, $\dot{M}_{\rm disk} \sim 10^{-4}\ M_\odot$ yr^{-1} (Hartmann & Kenyon 1996). In this model we have adopted a viscosity parameter $\alpha_{\rm disk} = 0.01$ (Whitney et al. 2003b). The disk accretion rate is directly proportional to the viscosity parameter (see eq. [4] in Whitney et al. 2003b); thus, a value of $\alpha_{\rm disk}$ of 0.1 would increase $\dot{M}_{\rm disk}$ by an order of magnitude (i.e., up to $10^{-6}\ M_\odot$ yr^{-1}) but provide the same match to the SED. Moreover, an increase of the disk accretion rate by a factor of about 3–5, for $\alpha_{\rm disk} = 0.01$, provides a match to the observed SED that, overall, is poorer than the one shown in Figure 4 and yields an $L_{\rm total}$ a factor of ~1.8–2.5 larger than the value derived integrating the SED, as in § 2.

The radiation transfer model fits satisfactorily the crude SED that we constructed for ISO-Cha I 192, suggesting that an infalling envelope + disk + central source configuration does provide a likely geometry for the system. We acknowledge, however, that a proper fit of such a complex two-dimensional model would require a more complete set of simultaneous observations, such as *Spitzer* IRS spectra supplemented by far-infrared and millimeter flux measurements, as well as high-resolution imaging in the near- and mid-infrared.

4. ISO-CHA I 192, A YOUNG FUor OR EXor SYSTEM

A number of the characteristics of ISO-Cha I 192 described here place this young star as a candidate member of the FUor or EXor class. The FUor systems are pre-main-sequence stars that undergo outbursts that amount to 4 or more magnitudes in V (Herbig 1977) and around 2–3 mag or more in K. On statistical grounds, it is believed that these outbursts are recurrent (occurring every $\sim10^5$ yr) throughout the lifetime of a T Tauri star. The eruptions are explained in terms of sudden increases in the accretion rate from a circumstellar disk into a central star, possibly caused by previous piling up of material in the disk. The brightening occurs in less than 1 yr and the luminosity of the system slowly (10–100 yr) decays, probably acquiring its preoutburst level again. In most cases, the FUor systems are associated with shocked H_2 knots and molecular outflows (Hartmann & Kenyon 1996 and references therein). The best-known examples (e.g., FU Ori and V1057 Cyg) are visibly bright young objects exhibiting large infrared excesses that evince the presence of dusty accretion disks. Their K-band spectra are characterized by CO absorption band heads, resembling late-type photospheres. A number of other highly embedded, much younger, class I FUor candidates have been proposed, and some of their observed characteristics seem to differ from the prototype objects. Being a recurrent phenomenon, it is not surprising that the detailed properties of the star, envelope, and disk vary from the very first eruptions, while being embedded class I objects, to those occurring at much later stages, as classical T Tauri stars.

Bona fide FUors show the CO 2.3 μm overtone in absorption (Kenyon & Hartmann 1989; Kenyon et al. 1993; Reipurth & Aspin 1997) that is expected to arise in Keplerian rotating circumstellar disk atmospheres (Calvet et al. 1991). A number of FUor-like candidates, on the other hand, do not display the CO absorption bands in the 2.3 μm region but exhibit other properties common to well-known FUors, such as sudden increases in luminosity, large infrared excesses, and association with outflows and shocked gas (Carr 1989; Hodapp et al. 1996; Reipurth & Aspin 1997, 2004; Vacca et al. 2004). In a few known cases, the CO bands are in emission.

The more ill-defined class of EX Lup or EXor systems are also classical T Tauri stars that undergo outbursts similar to those of FUors, although some of their differences (see, e.g., Aspin et al. 2006) are that the eruptions of the EXors appear to be of shorter duration (decaying more rapidly) and occur more frequently (on a timescale of decades) than those of FUors. After their outbursts, EXors seem to suffer greater short-term variability than FUors.

Many of the observed characteristics of ISO-Cha I 192 reported here do match those of FUors. Gómez & Mardones (2003) obtained a K-band spectrum of ISO-Cha I 192. The H_2 lines are in emission, superposed on a practically featureless and very steeply rising red continuum. In particular, no 2.3 μm CO band heads (neither in absorption or in emission) are seen in this relatively modest resolution ($R \sim 500$) near-infrared spectrum. As has been proposed for other embedded candidates (e.g., Serpens DEOS), these absorptions may be "veiled" by the rising dust continuum or probably filled by band emission. On the other hand, the observed photometric and spectroscopic behavior of ISO-Cha I 192 is also consistent with that of typical EXors.

It is interesting to compare the observed properties of ISO-Cha I 192 with those of the well-studied V1647 Ori. During their outbursts, both stars exhibited similar magnitude and color changes, $\Delta(J-H) \simeq -0.3$, $\Delta(H-K) \simeq -0.2$, and $\Delta K \simeq 1.9$ for ISO-Cha I 192 (see Table 2) and $\Delta(J-H) \simeq -0.5$, $\Delta(H-K) \simeq -0.3$, and $\Delta K \simeq 2.9$ for V1647 Ori (Vacca et al. 2004). Just after its outburst, the $(J-H)$ and $(H-K)$ color indices of the latter were 2.1 and 1.6, while those of ISO-Cha I 192 were 2.9 and 2.3, respectively. The comparison of their infrared spectra in several wavelength regions provides some interesting results. The H-band spectra of both sources are identical, showing rising continua with traces of very weak emission lines (Gómez & Mardones 2003; Vacca et al. 2004; Gibb et al. 2006). A deep 3.1 μm water ice

absorption feature is present in both, with the C-H stretching feature at 3.4 μm visible in the long-wavelength wing. Also present in their spectra is a moderate absorption at 4.67 μm assigned to CO ice. The Pfγ and Brα emission lines are also evident in both stars (Pontoppidan et al. 2003; Vacca et al. 2004; Gibb et al. 2006). The presence of an elongated reflection nebula in their close vicinities and extinctions amounting to $A_V \simeq 13$ are also common features.

On the other hand, the 2.0–2.5 μm spectra of our compared stars are extremely different. The spectrum of V1647 Ori shows prominently the 2.3–2.5 μm series of ^{12}CO ($\Delta v = 2$) bands in emission, together with Brγ and Na I lines (Vacca et al. 2004; Gibb et al. 2006). In contrast, the spectrum of ISO-Cha I 192 obtained by Gómez & Mardones (2003) shows strong emission of the 2.4–2.5 μm H_2 Q series and the 2.12 μm $H_2(1-0)$ line and no Brγ or CO bands, either in emission or absorption. In the case of ISO-Cha I 192, the available K-band spectrum was obtained on 1999 April 10 and 12, when the eruption was probably in course (see Table 2 and Fig. 1). The lack of absorption in the CO bands may be a temporary feature. Finally, no silicate 9.7 μm emission or absorption is present in the spectrum of V1647 Ori (Ábrahám et al. 2006), while our mid-infrared narrowband photometry reveals this feature in absorption.

There has been controversy in the literature as to whether V1647 Ori belongs to the EXor or FUor class (e.g., Reipurth & Aspin [2004] vs. Briceño et al. [2004]), as the star shows a number of characteristics that can be fitted to either class. We support the statement by Aspin et al. (2006) in the sense that, at present, "given our limited understanding of either group of stars, it is still unclear whether this is a semantic distinction, i.e., whether FUors and EXors are different shades of the same phenomenon." Clearly, the validity of this statement is enhanced when applied to ISO-Cha I 192, which has very limited observational data available. One important point in this respect is that the model fitted to our SED yields a disk accretion rate of the order of $10^{-7}\ M_\odot\ \mathrm{yr}^{-1}$, some 3 orders of magnitude lower than the canonical values for the disk accretion rates derived for bona fide FUors.

The above comparison illustrates well the differences in the detailed observable characteristics of these kinds of young eruptive objects. It is well known that similar contrasting features are seen even among accepted bona fide FUor systems (Hartmann & Kenyon 1996). Furthermore, certain spectroscopic properties are dependent on how advanced in its eruption a particular object is observed (e.g., V1057 Cyg; Briceño et al. 2004). Clearly, the observed properties of each eruptive system (spectrum, SED, variability, etc.) depend on the precise physical intrinsic and environmental conditions under which the outburst occur, not to mention geometric factors, most notably the inclination angle of the disk. Therefore, it should not be surprising to find such varying spectroscopic "signatures" in different confirmed FUors and FUor-like objects, and also in EXors. Note, for example, that the 9.7 μm silicate feature is seen in many of these objects either in emission or absorption, and in other cases it is totally absent (Schütz et al. 2005). If, as is commonly accepted, the FUor and EXor phenomena are recurrent in the life of pre-main-sequence low-mass stars, it would be natural to expect detailed differences in each sequential eruption, and thus, these may be the result of evolutionary effects, both in the star and its disk. We could even imagine that FUors and EXors are consequences of the same physical phenomenon, only with one occurring much later in the life of a T Tauri star. Evolutionary effects could be responsible for making the decay time much faster in EXors than in FUors.

5. SUMMARY

We report the detection of a brightness increase of about 2 mag in the K_s-band magnitude of ISO-Cha I 192, a class I object thought to be driving a bipolar CO outflow in the Chamaeleon dark cloud. This substantial change has occurred during a period of about 3 yr, from March 1996 until April 1999, although the eruptive event may have occurred in a much shorter period.

New ground-based and satellite observations of ISO-Cha I 192 are presented in the wavelength range 2–70 μm. These include calibrated images taken with the Clay/Magellan telescope at Las Campanas and the ESO 3.6 m telescope at La Silla, and archive IRAC and MIPS images taken with *Spitzer*.

During the eruption, the object has a luminosity $L \geq 1.5\ L_\odot$, implying a very low mass pre-main-sequence star. An elongated infrared reflection nebula of size $\sim$530 AU is seen originating from the star in the direction of the CO bipolar outflow.

Many of the properties that we found in ISO-Cha I 192, notably the large outburst, association with shocked molecular hydrogen, and certain spectroscopic features, suggest that this is a very young eruptive. Its observed characteristics are similar to known FU Ori– or EX Lup–type systems, although the implied low mass and low accretion rate support the latter case.

We have combined quasi-simultaneous photometry from the literature with new mid-infrared data reported in this contribution to construct the SED of this object. We used a two-dimensional radiative transfer code that adopts a realistic configuration for the young star, including the contributions of an infalling envelope, a flared disk, and bipolar cavities (Whitney et al. 2003a, 2003b). This model fits the observed SED reasonably well in the infrared regimen. However, this modeling attempt ought to be taken as an experiment.

We are grateful to the ESO and Las Campanas staff for assistance during the observing runs. We also thank Antonella Natta for helpful comments and suggestions throughout this project. This research has made use of the SIMBAD database, operated at CDS, Strasbourg, France. This publication makes use of data products from the Two Micron All Sky Survey, which is a joint project of the University of Massachusetts and the Infrared Processing and Analysis Center/California Institute of Technology, funded by the National Aeronautics and Space Administration and the National Science Foundation. M. T. acknowledges UNAM/DGAPA grant IN102803.

REFERENCES

Ábrahám, P., Mosoni, L., Henning, T., Leinert, C., Quanz, S. P., & Ratzka, T. 2006, A&A, 449, L13
Andrews, S. M., & Williams, J. P. 2006, ApJ, 631, 1134
Aspin, C., Barbieri, C., Boschi, F., Di Mille, F., Rampazzi, F., Reipurth, B., & Tsvetkov, M. 2006, AJ, 132, 1298
Aspin, C., & Reipurth, B. 2003, AJ, 126, 2936
Batalha, C. C., et al. 1998, A&AS, 128, 561
Beckwith, S. V. W., Sargentenvirinmental, A. I., Chini, R. S., & Guesten, R. 1990, AJ, 99, 924
Briceño, C., et al. 2004, ApJ, 606, L123
Calvet, N., Hartmann, L., & Kenyon, S. J. 1991, ApJ, 383, 752
Cambrésy, L., Copet, E., Epchtein, N., de Batz, B., Borsenberger, J., Fouque, P., Kimeswenger, S., & Tiphene, D. 1998, A&A, 338, 977
Carpenter, J. M., Hillenbrand, L. A., Skrutskie, M. F., & Meyer, M. R. 2002, AJ, 124, 1001
Carr, J. S. 1989, ApJ, 345, 522
Cotera, A. S., et al. 2001, ApJ, 556, 958
D'Antona, F., & Mazzitelli, I. 1994, ApJS, 90, 467

Gibb, E. L., Rettig, T. W., Brittain, S. D., Wasikowski, D., Simon, T., Vacca, W. D., Cushing, M. C., & Kulesa, C. 2006, ApJ, 641, 383
Gómez, M., & Kenyon, S. 2001, AJ, 121, 974
Gómez, M., & Mardones, D. 2003, AJ, 125, 2134
Gómez, M., Persi, P., Marenzi, A. R., Roth, M., & Tapia, M. 2004, A&A, 423, 629
Hartmann, L., & Kenyon, S. J. 1996, ARA&A, 34, 207
Herbig, G. H. 1977, ApJ, 217, 693
Herbig, G. H., Aspin, C., Gilmore, A. C., Imhoff, C. L., & Jones, A. F. 2001, PASP, 113, 1547
Herbst, W., Herbst, D. K., Grossman, E. J., & Weinstein, D. 1994, AJ, 108, 1906
Hodapp, K.-W., Hora, J. L., Rayner, J. T., Pickles, A. J., & Ladd, E. F. 1996, ApJ, 468, 861
Hogerheijde, M. R., & Sandell, G. 2000, ApJ, 534, 880
Jones, T. J., Hyland, A. R., Harvey, P. M., Wilking, B. A., & Joy, M. 1985, AJ, 90, 1191
Jorgensen, J. K., Schoier, F. L., & van Dishoeck, E. F. 2002, A&A, 389, 908
Kainulainen, J., Lehtinen, K., & Harju, J. 2006, A&A, 447, 597
Kenyon, S. J., & Hartmann, L. 1987, ApJ, 323, 714
———. 1989, ApJ, 342, 1134
Kenyon, S. J., Hartmann, L., Gómez, M., Carr, J. S., & Tokunaga, A. 1993, AJ, 105, 1505
Kenyon, S. J., Yi, I., & Hartmann, L. 1996, ApJ, 462, 439
Mattila, K., Liljeström, T., & Toriseva, M. 1989, in Low-Mass Star Formation and Pre-Main-Sequence Objects, ed. B. Reipurth (Garching: ESO), 153
Mizuno, A., Hayakawa, T., Tachihara, K., Onishi, T., Yonekura, Y., Yamaguchi, N., & Kato, S. 1999, PASJ, 51, 859
Movsessian, T. A., Khanzadyan, T., Aspin, C., Magakian, T. Y., Beck, T., Moiseev, A., Smith, M. D., & Nikogossian, E. H. 2006, A&A, 455, 1001
Oasa, Y., Tamura, M., & Sugitani, K. 1999, ApJ, 526, 336
Osterloh, M., & Beckwith, S. V. W. 1995, ApJ, 439, 288
Padgett, D. L., Brandner, W., Stapelfeldt, K. R., Strom, S. E., Terebey, S., & Koerner, D. 1999, AJ, 117, 1490
Persi, P., Marenzi, A. R., Kaas, A. A., Olofsson, G., Nordh, L., & Roth, M. 1999, AJ, 117, 439
Persson, S. E., Murphy, D. C., Krzeminski, W., Roth, M., & Rieke, M. J. 1998, AJ, 116, 2475
Pontoppidan, K. M., Dartois, E., van Dishoeck, E. F., Thi, W.-W., & d'Hendecourt, L. 2003, A&A, 404, L17
Reipurth, B., & Aspin, C. 1997, AJ, 114, 2700
———. 2004, ApJ, 606, L119
Reipurth, B., Yu, K. C., Heathcote, S., Bally, J., & Rodriguez, L. F. 2000, AJ, 120, 1449
Sandell, G., & Aspin, C. 1998, A&A, 333, 1016
Sandell, G., & Weintraub, D. A. 2001, ApJS, 134, 115
Schütz, O., Meeus, G., & Sterzik, M. F. 2005, A&A, 431, 165
Skrutskie, M. F., Meyer, M. R., Whalen, D., & Hamilton, C. 1996, AJ, 112, 2168
Stassun, K., & Wood, K. 1999, ApJ, 510, 892
Tapia, M., Persi, P., Bohigas, J., & Ferrari-Toniolo, M. 1997, AJ, 113, 1769
Vacca, W. D., Cushing, M. C., & Simon, T. 2004, ApJ, 609, L29
Whitney, B. A., Wood, K., Bjorkman, J. E., & Cohen, M. 2003a, ApJ, 598, 1079
Whitney, B. A., Wood, K., Bjorkman, J. E., & Wolff, M. J. 2003b, ApJ, 591, 1049